Fracto-emission from deuterated titanium: Supporting evidence for a fracto-fusion mechanism

J.T. Dickinson, L.C. Jensen, and S.C. Langford
Washington State University, Pullman, Washington 99164-2814

R.R. Ryan and E. Garcia
Los Alamos National Laboratory, Los Alamos, New Mexico 87545

(Received 14 July 1989; accepted 31 August 1989)

Measurements of the emission of charged particles, photons, and radio frequency signals accompanying the deformation and fracture of polycrystalline Ti metal and deuterated Ti are described. Preliminary evidence for charge separation created by crack propagation is presented which supports a proposed fracture mechanism to explain neutron bursts observed during treatment of deuterated metals.

I. INTRODUCTION

The reported observations of fusion accompanying electrochemical loading of deuterium into Pd and Ti by Fleischmann and Pons[1] and by Jones *et al.*[2] stimulated experiments involving the detection of neutrons during treatment of both gas loaded and electrochemically loaded specimens of these metals. Scaramuzzi *et al.*[3] and Menlove *et al.*[4] showed that heating and/or cooling metal specimens exposed to high pressure D_2 frequently resulted in statistically significant bursts of neutrons. We,[5] Cohen and Davies,[6] Mayer *et al.*,[7] Furth,[8] and Segre *et al.*[9] have independently proposed a mechanism leading to a D + D fusion reaction involving crack propagation in the embrittled material. A schematic of the model is shown in Fig. 1. We suggest that crack growth results in charge separation on the newly formed crack surfaces, which act like a miniature "linear accelerator;" i.e., D^+ ions are accelerated in the electric field across the crack tip to kinetic energies of $10–10^4$ eV or more, sufficient to raise significantly the D + D fusion probability. An important requirement of this model is that during fracture and because of fracture, D^+ exists as a free ion in the volume of the crack. We refer to this proposed fracture-induced fusion mechanism as *fracto-fusion*. It should be noted that Deryagin *et al.* have published the observation of neutron bursts accompanying impact loading of LiD and described a similar crack acceleration model.[10,11]

In previous work on particle emission accompanying fracture (so-called fracto-emission) we have observed that a number of materials (see Refs. 12–19) exhibit intense charged particle and photon emission as well as bursts of radio frequency signals upon fracture, indicating charge separation across the crack (i.e., separating charge patches are equivalent to rapid current variations), sometimes accompanied by small but consistent microdischarges which produce broad band, far field electromagnetic radiation. Strong charge separation effects are most often observed in piezo- or ferro-electric materials, layered structures, and in adhesively bonded interfaces where bond breaking occurs in a state of high polarization. Examples of each are fracture of single crystal quartz, electrically polarized lead zirconate titanate, mica, and polymer-metal interfaces. All of these materials produce intense fracto-emission and easily detected radio frequency emission. Note that all of these systems involve components that are good insulators so that separated charge is not readily neutralized on timescales of at least several microseconds (duration of fracture). In addition to emission during fracture, these materials exhibit sustained emission, sometimes for as long as 2 h following fracture, due to excitations resulting from charged particle bombardment of the insulating fracture surfaces. Very similar "tails" in the emission can be generated by bombarding insulator surfaces with energetic electrons.[19] This process is analogous to the thermally stimulated luminescence and electron emission observed following exposure of insulators to radiation.[20]

In the case of metals, we have observed that polycrystalline Al, when freed of surface oxide and fractured in ultrahigh vacuum, yields little or no emission.[21,22] Although metallic bonds are being broken and stochastic distributions of charge on the fracture surfaces are possible, high conductivity should result in decay times on the order of 10^{-14} s, making charge acceleration in the crack unlikely. Mayer has suggested that longer decay times might result from crack geometry.[7] Perhaps more importantly, impurity segregation and the existence of inclusions in commercial metals and alloys may result in interfaces and insulating surface layers that simultaneously induce strong charge separation and inhibit reneutralization at separating fracture surfaces for considerably longer times. Because of the current interest in these effects, we felt it appropriate to make a preliminary study of the fracto-emission from deuterated Ti. In this paper, we present measurements of negative and

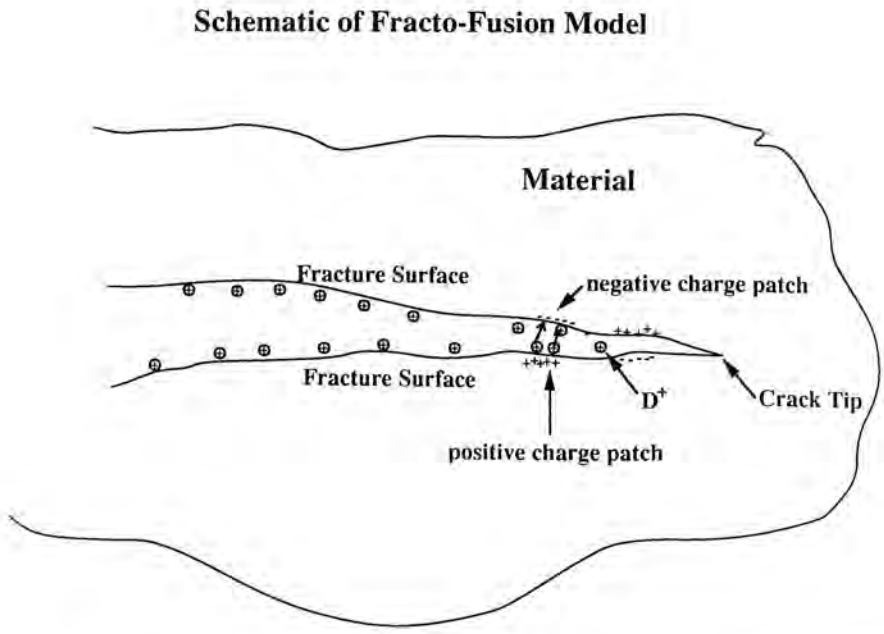

FIG. 1. Schematic diagram of the fracto-fusion model where a propagating crack produces separation of charge and releases D^+ which accelerates in the resulting **E** field, thereby enhancing the D + D fusion reaction.

positive charge emission, visible photon emission, radio frequency emission, and preliminary mass spectroscopy of a single neutral species emitted during and following deformation and fracture of deuterated Ti. A number of these observations provide supporting evidence for a fracto-fusion mechanism.

II. EXPERIMENTAL

Details of our experimental arrangements can be found in Refs. 12–19. The majority of the experiments shown here were performed in vacuum at 10^{-6} Torr in a system containing a large O-ring in a removable top. We discovered after the completion of these experiments that there may have been a small leak associated with this seal during these studies, implying that there might have been a small partial pressure of molecular oxygen in the background. Charge particles were detected with Galileo Electro-optics Corporation Channeltron electron multipliers, which produce fast (10 ns) pulses with high detection efficiency for both electrons and $\pm$ ions. Background noise count rates typically ranged from 1 to 10 counts/s. The detectors were positioned 1–2 cm from the sample, with the bias voltage on the front cone chosen to attract the charged particles of interest. It should be noted that in a number of fracto-emission studies, we have shown that the principal particles detected for positive and negative bias on the Channeltron front cone are electrons and positive ions, respectively.

Photons were detected with a Thorn-EMI 9924QB photomultiplier tube also mounted inside the vacuum system. This photomultiplier responds to photons of wavelengths from about 600 nm to 200 nm, with a maximum quantum efficiency of 25%. Within the vacuum system cooling the photomultiplier was not practical, resulting in relatively high backgrounds of typically 1000 counts/s.

Radio frequency emission was detected with coil antennas placed a few mm from the sample. Such an antenna couples to a changing B field. It should be emphasized that with the antenna only a few mm from the sample, one detects the *near-field* electromagnetic "emission" because of the close proximity of the coils to the source. Thus, moving charge (e.g., due to charge separation) can be detected by such a probe. Simultaneous emission of visible photons and radio frequency bursts is indicative of actual microdischarges occurring in the crack. The most unambiguous fracture experiments where discharges have been detected are in systems involving interfacial failure.

Neutral particles were detected with a UTI 100C quadrupole mass spectrometer, tuned to a single mass peak. The spectrometer is equipped with an ionizer, in which neutrals are ionized by electron impact at an energy of 70 eV. Mass spectrometry was performed in an ultra-high vacuum system with base pressures on the order of 5×10^{-9} Torr.

Samples were cut to $12 \times 6 \times 1.6$ mm^3 from commercial Ti sheet and degassed by heating in vacuum to 750 °C for 1 h. The chamber was then backfilled with the appropriate gas (H_2 or D_2) at 100 Torr and the samples slowly cooled to 400° over a period of an hour and a half, maintaining the 100 Torr. The samples were finally quenched to room temperature. The degree of loading was determined from the weight increase which occurred during hydration/deuteration. The resulting

H:Ti ratio was about 1.0. The D:Ti ratio was typically somewhat lower, about 0.8, due to the lower diffusivity of D relative to H in the Ti lattice. The process of hydration/deuteration yielded quite brittle samples which were readily fractured in three-point bend using devices compatible with high or ultra-high vacuum. Typical loading rates were 10–50 μm/s. Unhydrated/undeuterated "dogbone" samples were prepared from 0.5 mm commercial Ti sheet subjected to the same thermal cycling as the hydrated/deuterated samples, but without backfilling the vacuum system during the cooling step. These samples were notched to ensure that fracture occurred near the detectors and loaded in tension at an elongation rate of ~40 μm/s (~0.60%/s). The tension geometry can accommodate the much larger plastic deformation associated with unhydrated/undeuterated samples.

Figure 2(a) shows a schematic of the detector arrangements for simultaneous photon and charged particle detection. When better collection geometry was desired, the sample holder was rotated 90° so that the crack opened directly in front of a single detector, as shown in Fig. 2(b), where the "single detector" = photomultiplier, Channeltron, or quadrupole mass spectrometer. In the case of charged particle detection, this orientation increased the electric field at the sample surface and consequently greatly improved the collection efficiency of the Channeltron cone. An acoustic emission transducer (Acoustic Emission Technology Corp. AC1500L) was attached to the breaker to provide a time marker and trigger pulse associated with the fracture event. Signals were either pulse counted with a multichannel scaler or digitized at 10 ns/channel.

III. RESULTS AND DISCUSSION

Weight measurements made before and after fracture showed no evidence of weight loss at the 0.1 mg level due to exposure to the vacuum and/or fracture; thus, the TiD_x and TiH_y compounds formed were quite stable on this macroscopic level.

Figure 3 shows the detected signals (counts/10 ms time interval) for a TiD_x specimen (where $x \sim 0.8$). The Channeltron cone was biased at +300 V and the Channeltron and photomultiplier were positioned as shown in Fig. 2(a). Similar samples tested in the same geometry but with higher positive cone voltages showed significant increases in count rate; this strongly suggests that negatively charged particles are indeed being collected. We do not know for certain that these are electrons and therefore refer to these emissions as negative charge emission; however, for a large number of other materials, negative charge emission is dominated by electron emission and we suspect that this is also the case for these samples. Of several samples fractured in this manner, the basic time dependence for both the negative charge and photon emissions was similar to the data

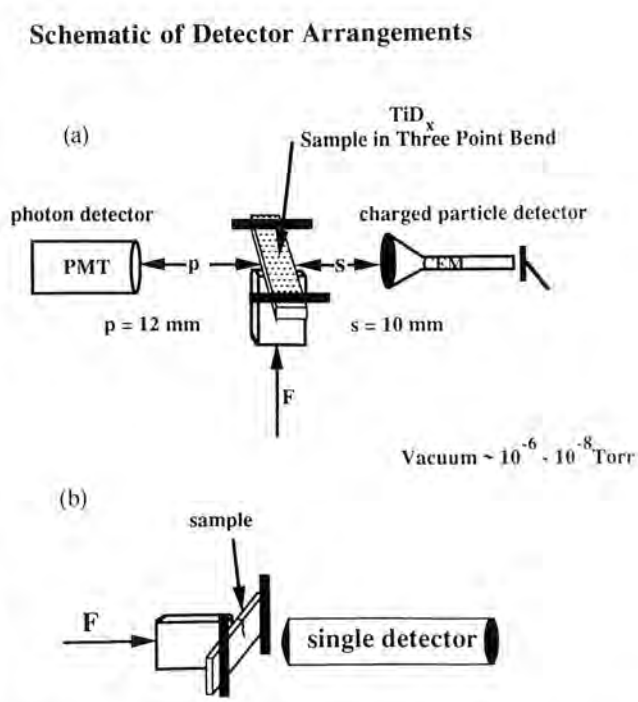

FIG. 2. Schematic of detector arrangement for simultaneous measurements on charged particle and photon emission. When improved sensitivity was desired, the breaker could be rotated 90° so that the crack opened directly toward the chosen detector, shown in (b).

shown in Fig. 3: a distinct peak at fracture (shown by the arrows) is followed by what appears to be a relaxation-type tail lasting several seconds. Note that despite the high noise level in the photon emission prior to fracture, the photon emission appears to parallel the negative charge emission for some time after fracture.

Figure 4 represents a similar experiment with the front cone of the Channeltron at −2200 V. Such voltage should repel all but the most energetic negatively charged particles. In this particular data set, the photon emission returned to the noise level very rapidly after fracture.

To be absolutely sure that positive ions are indeed emitted, we arranged the Channeltron in the configuration shown in Fig. 5(a), where a metallic disk at ground potential shadowed the Channeltron from line of sight of the crack. Any excited neutral particle would be stopped by the disk, any negatively charged particle would be deflected away from the detector, and any positively charged particle would be detected if it could be drawn around the disk due to the −2200 V on the Channeltron cone. Although the resulting detected emission was small due to constraints, we see in Fig. 5(b) a significant peak at fracture with a few channels of after-emission. We therefore have strong evidence that positive ion emission is produced by fracture of this material. If D^+ is indeed a component of this positive charge emission, then a crucial requirement for the fracto-fusion model, namely free D^+ in the crack, would be met.

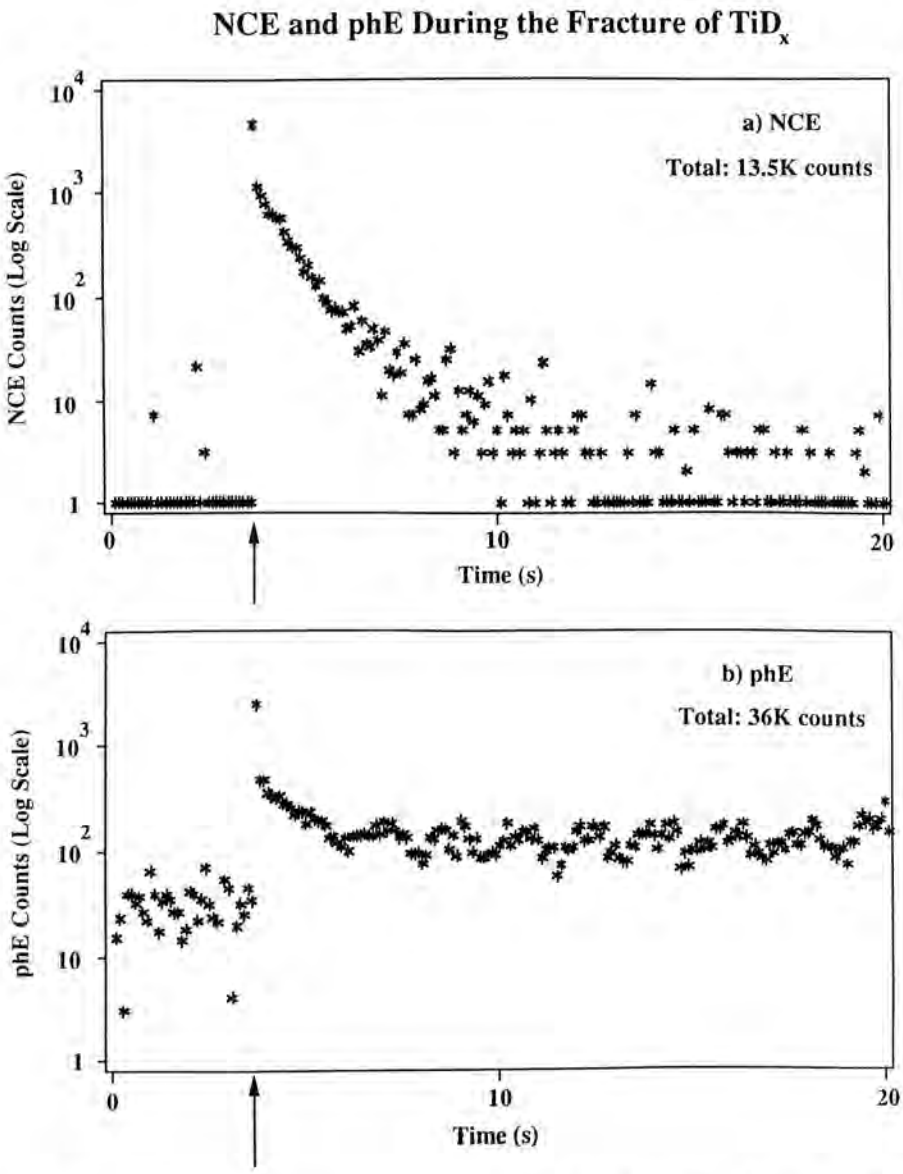

FIG. 3. Simultaneous measurements of (a) negative charge emission (NCE) and (b) photon emission (phE) from the fracture of a TiD_x sample broken in three point bend [Fig. 2(a) geometry].

When the specimen is rotated so as to break directly facing the Channeltron, considerably more negative charge and positive ion emissions are collected. Figure 6 shows the resulting counts/channel (10 ms/channel) versus time for this geometry (no beam block in position) with the Channeltron front cone biased at (a) +300 V, thus attracting negative charge, and (b) −2200 V, thus attracting positive charge. The negative charge emission [Fig. 6(a)] at fracture begins to decay immediately, reaches a minimum, then grows to a broad peak in a few seconds, followed by a nearly exponential decay (similar to Fig. 3) lasting many tens of seconds (the inset shows 80 s of the same data taken at 160 ms/channel). The positive charge emission [Fig. 6(b)] has multiple peaks at and following failure, possibly due to crack arrest and resumed crack growth. The tail after fracture was weak, lasting a few seconds, and appeared to be unrelated to the negative charge emission.

The behavior of the negative charge emission appears suspiciously like a phenomenon known as chemisorptive electron emission[23–26] where a clean metal surface with relatively low work function reacts with gases such as O_2, halogens, and perhaps H_2O during chemisorption. This reaction induces nonadiabatic electronic transitions that result in both chemisorptive luminescence and electron emission. Models developed by Norskov *et al.*,[27] Kasemo *et al.*,[28] and Prince *et al.*[29] describe a strong work function dependence and predict that as coverage increases, the emission rate decreases. Born and Linke[30] have reported dramatic work function decreases on Al surfaces, for example, due to H_2O adsorption. H_2O is a significant component of the background gases in our vacuum system.

In our case, deformation and fracture would produce an increasing number of clean metal sites (recall that not all of the Ti metal has reacted with D). After fracture,

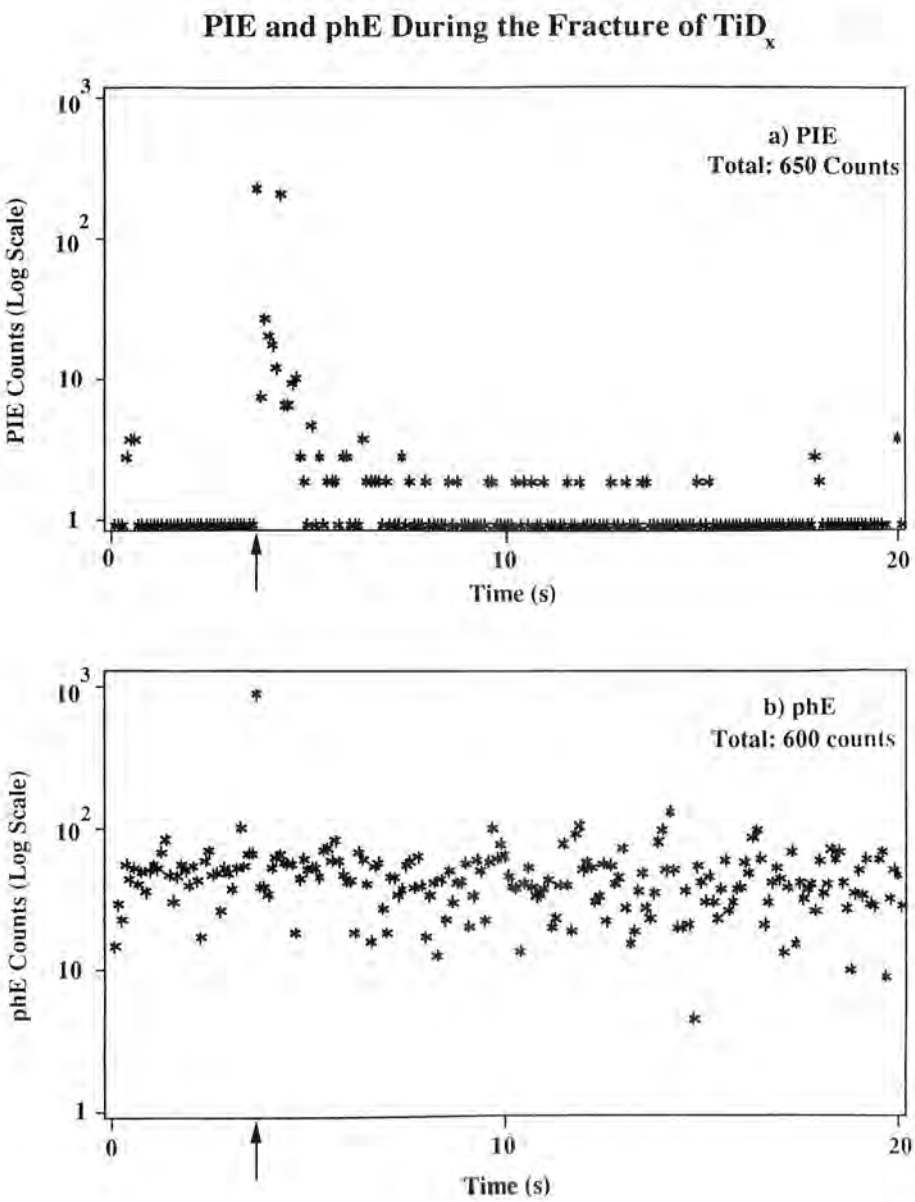

FIG. 4. Simultaneous measurements of (a) positive ion emission (PIE) and (b) photon emission (phE) from the fracture of a TiD_x sample broken in three point bend [Fig. 2(a) geometry].

chemisorption begins on the clean metal sites as soon as the gas can reach the surface. Assuming the reaction probability is proportional to the number of remaining clean metal sites, an exponential decay in emission rate would be observed, consistent with the *later* times (after a few seconds) in the observed emission. If at low coverages, chemisorption decreases the work function of the surface, the emission rate would in fact increase at the onset, thus explaining the observed secondary maximum emission rate following fracture. Several deuterated specimens showed photon emission after fracture which paralleled the negative charge emission, consistent with a parallel chemisorptive luminescence mechanism.

To test this hypothesis, we performed tensile tests on undeuterated Ti tensile specimens in background vacuum and during exposure to O_2 at a pressure of $\sim 10^{-5}$ Torr; O_2 is known to induce chemisorptive luminescence and electron emission on a number of metals, including Ti. If a significant change in the photon and electron emissions is observed during elongation and fracture, this would indicate that chemisorptive luminescence and electron emission could explain these after-emission curves. Figure 7 compares the negative charge and photon emissions for these two atmospheres. We first note that the undeuterated Ti in background vacuum still emits both negative charge and photons at fracture; furthermore, the total emission was of the same order of magnitude as the brittle deuterated Ti broken in three point bend. The O_2 atmosphere is associated with much more intense negative charge and photon emissions than the background vacuum, particularly in the case

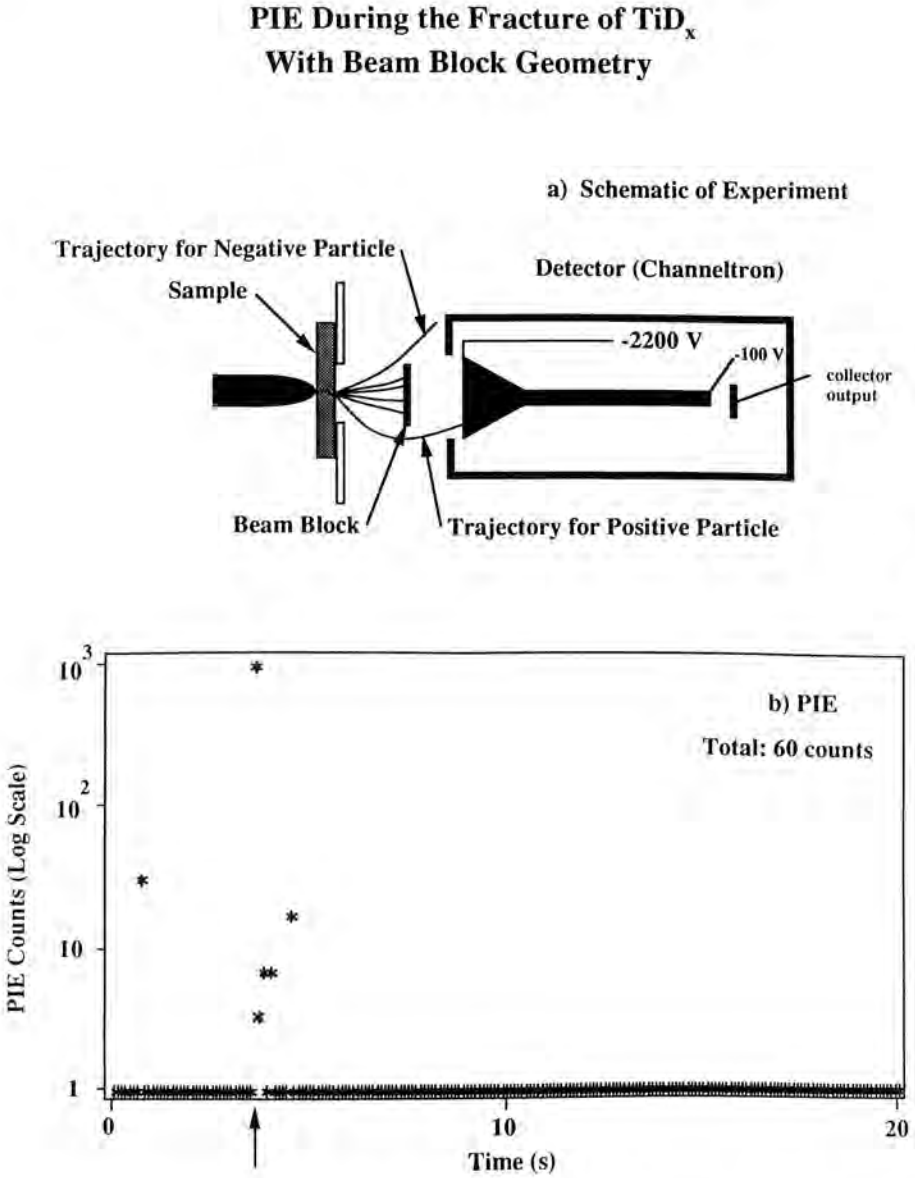

FIG. 5. (a) Experimental configuration for verification of emission of positively charged particles by use of a beam block mounted between the specimen and the detector. (b) The resulting positive ion emission (PIE) from TiD_x.

of negative charge emission. The secondary maximum observed in the negative charge emission (and to some extent in the photon emission) immediately after fracture in the background vacuum is not observed in the O_2 atmosphere. The partial pressure of active gases is at least 2 orders of magnitude higher in the O_2 ambient than in the background vacuum, greatly reducing the time required for establishing intense chemisorptive emissions. Thus, the time to form this secondary peak is too small to be resolved by the rate of data acquisition employed in Fig. 7. The negative charge emission prior to fracture is evident in both background and the O_2 atmosphere, where it is greatly enhanced. These emissions are due to plastic deformation (extensive in the undeuterated material) which brings clean Ti metal (via step formation) to the surface where it reacts with the active gases. The resulting chemisorptive electron emission rate depends on the rate at which fresh Ti reaches the surface and the rate of chemisorption (which is often strongly dependent on gas surface coverage). For the two specimens shown, the negative charge emission intensities can be divided in time as follows:

	Counts during 80 ms time interval including fracture event	Integrated counts in tail ~30 s time interval
In background	1.3 K	95 K
In O_2	50 K	23 K

The total counts for these two negative charge emission curves are approximately the same; assuming that the surface areas of clean Ti metal created are equal in the two samples, then the total chemisorptive electron emissions would be expected to be nearly equal.

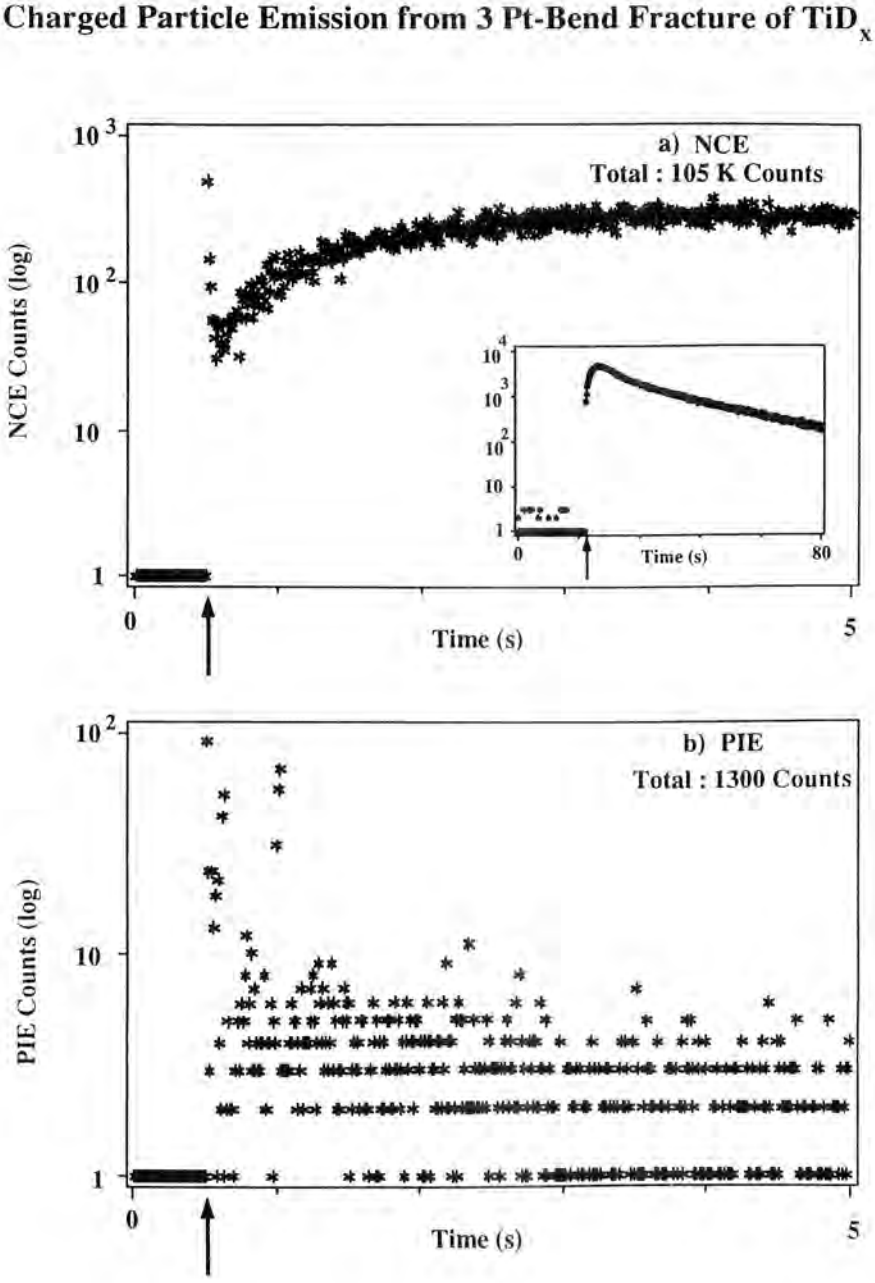

FIG. 6. The charged particle emission for two different TiD_x samples where the specimen is loaded in three point bend [Fig. 2(b) geometry]. The Channeltron electron multiplier is biased for (a) detection of negative charge emission (NCE) and (b) detection of positive ion emission (PIE). The inset displays the negative charge emission data over a longer time interval.

One characteristic of almost all of the negative charge emission data presented so far is the two types of kinetics controlling the after-emission (following the secondary maximum): (i) a first order decay (in background: $\tau \sim 8$ s; in 10^{-5} Torr O_2: $\tau \sim 0.05$ s), and (ii) a nearly steady, low count rate emission. The decay represents chemisorptive electron emission responding in a first order fashion to a fixed number of available chemisorption sites in two different partial pressures of reactive gas; the ratio of the time constants is inversely proportional to the partial pressure (about a factor of 160), which predicts a quite reasonable value for the O_2 partial pressure in the background vacuum, if we assume that O_2 in the background gas is due to a small leak. The nearly constant emission is consistent with a steady state process wherein O chemisorption sites are made continuously available, e.g., through replacement of $O_{chemisorbed}$ by reaction and desorption with background CO or H_2. The products (CO_2 or H_2O) would desorb, leaving a clean adsorption site. Obviously, many of these questions can be resolved by moving the experiment into ultrahigh vacuum, which we plan to do in the near future.

A very important question in relation to the fracto-fusion mechanism is: Are there negative charge and photon emission components unattributable to chemisorp-

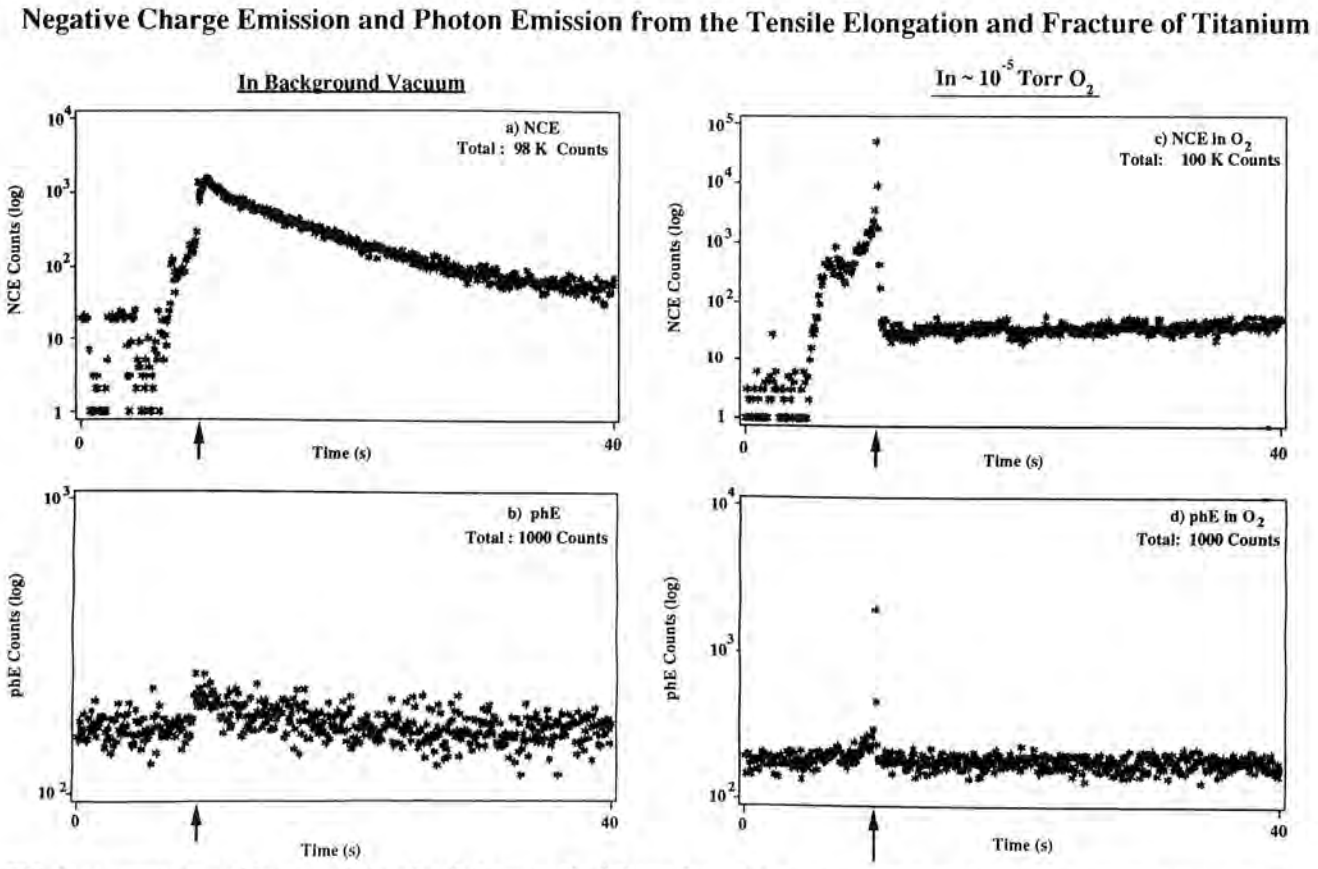

FIG. 7. A comparison of fracto-emission signals from tensile deformation and fracture of commercial Ti in background vacuum: (a) negative charge emission (NCE) and (b) photon emission (phE); and in $\sim 10^{-5}$ Torr O_2: (c) negative charge emission and (d) photon emission.

tive electron emission and luminescence? Such emission should be most readily apparent during and shortly after fracture, while chemisorptive electron emission and luminescence processes are still quite weak. Examples of this faster emission are shown in Figs. 8(a) (negative charge emission) and 8(b) (positive ion emission) for two different deuterated Ti specimens fractured in three point bend, where we display the digitized Channeltron output. The data were acquired at 10 ns/channel over a total time of 800 μs and integrated over successive 1 μs time intervals; the location of the first fracture event as determined from the acoustic emission trigger pulse is indicated by the arrow. One sees that in both cases the emission was relatively concentrated in two bursts with approximately the same duration and time between the bursts. The smaller, more scattered signals seen at other times correspond to single particles striking the detector. Similar behavior (two bursts) was frequently observed in the photon emission. One is tempted to attribute these bursts to multiple fracture events (crack arrest), although the time interval between the bursts is rather long. These emissions decay rapidly (1–2 ms) and merge into the chemisorptive emission which is at a much lower rate and gradually increases with time, as described above, on time scales of 0.01–1 s. Thus, the processes responsible for chemisorptive electron emission long after fracture are not likely responsible for these bursts of emissions during and shortly after fracture.

As a preliminary test of possible electrostatic activity accompanying these fast fracto-emission features, we placed a small coil around the end of the photomultiplier so that radio frequency and photon emissions could be detected simultaneously. The response of this "antenna" to a burst of radio frequency B-field consists of a damped ringing signal resonating at the resonant frequency of the LCR circuit associated with the coil and amplifier (264 kHz). In the past, such correlations have served as a test for either charge separation or microdischarges accompanying fracture. Radio frequency and photon emissions accompanying the fracture of TiD_x in vacuum are shown in Fig. 9. Note the different timescales for the two signals; the time of fracture is marked by the arrows. The existence of such a radio frequency signal strongly supports the presence of charge separation. In past work, supporting evidence for microdischarges accompanying fracture involved intense photon emission *during* fracture accompanying such radio frequency signals. Relative to other materials which dis-

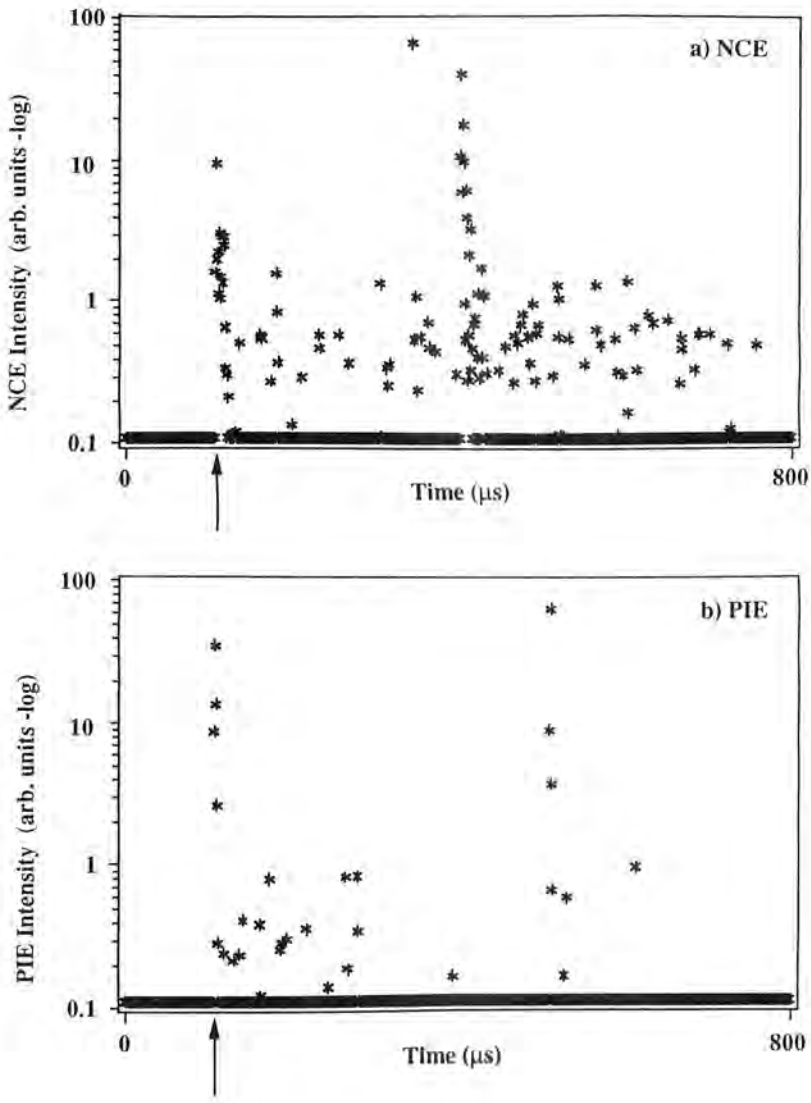

FIG. 8. Charged particle emission acquired on a faster timescale from the fracture of two different TiD_x samples in three point bend. The resulting (a) negative charge emission (NCE) and (b) positive ion emission (PIE) show two fairly intense bursts which may be due to multiple fracture events.

play microdischarges, the photon emission burst at fracture in Fig. 9 is quite small and seems to be spread out over several hundred μs. Although the radio frequency signal is clear evidence for electrical activity, the observed radio frequency and photon emissions are probably not due to microdischarges in the crack.

The nature of this electrical activity was further investigated by testing for the generation of electrical currents during and following fracture. The sample was electrically isolated from the three point bend apparatus and wired in series with the 50 Ω input resistor of an amplifier so that fracture would cut the circuit between one end of the sample, connected to ground, and the other end of the sample, tied to the amplifier input resistor (see diagram of the circuit shown in the inset of Fig. 10). It is important to note that initially both ends of the sample were at ground potential, and no external potential or field was applied to the circuit during the course of the experiment. Figure 10 shows the digitized amplifier output, converted to current (i = V/R), during the fracture of a TiH_x sample (used in place of TiD_x due to sample availability at the time). At or soon after fracture, as determined by an accompanying acoustic emission source, a rapidly fluctuating voltage is recorded. The fluctuations are consistent with variations in the charge balance across the crack tip during fracture. After ~15 μs, a sharp drop in signal (negative current) is observed, followed by a slow decay toward zero. Any charge imbalance remaining across the crack following failure is expected to yield a rapid falling (or rising) current followed by a super-exponential decay as the two sides of the crack accelerate away from each other.

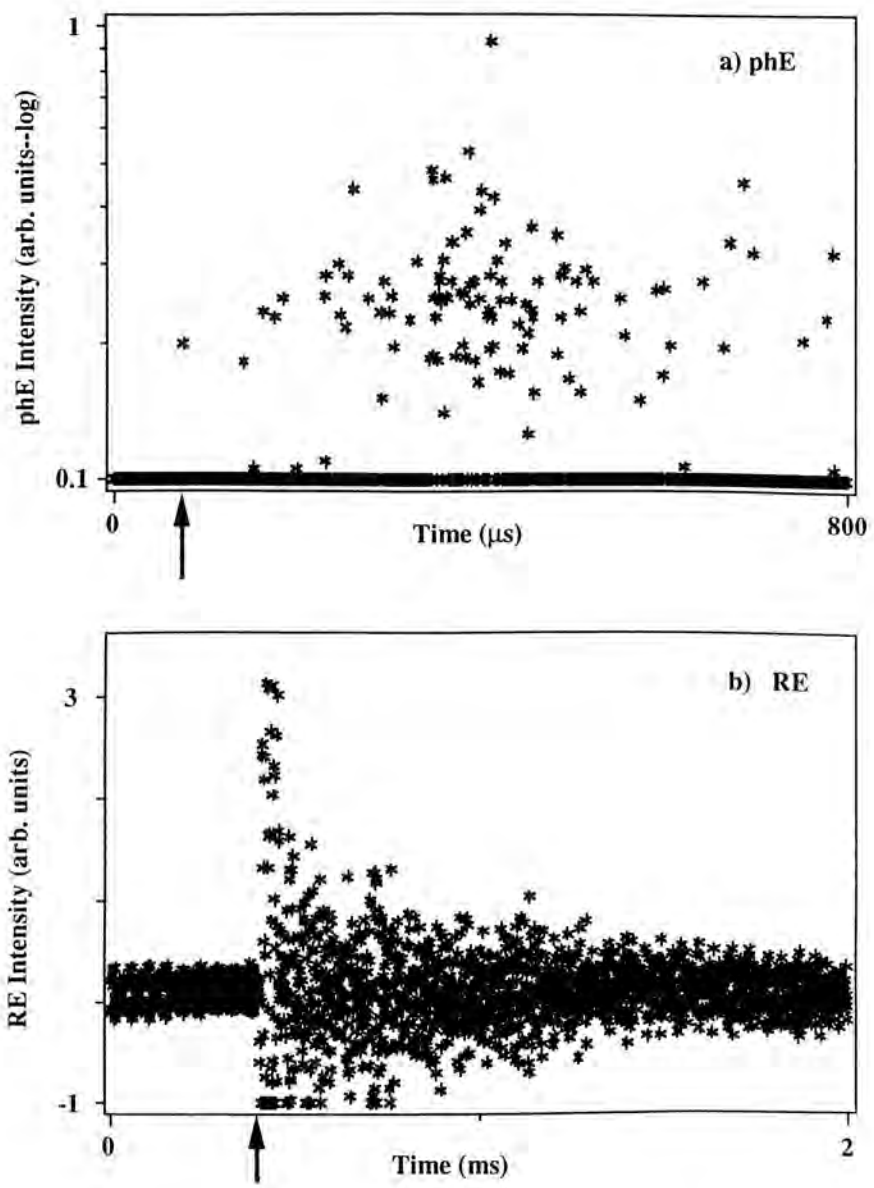

FIG. 9. Simultaneous measurements of (a) photon emission (phE) and (b) radio frequency emission (RE) produced by fracture of TiD_x in vacuum. The radio frequency signal is a damped, ringing signal responding to an "impulse" of changing **B** field at fracture.

The decay is punctuated by occasional ringing signals, perhaps due to the influence of reflected acoustic waves on the path of the separating pieces of sample. Although we cannot absolutely rule out the presence of artifacts in this signal, our attempts to explain these signals on the basis of anything other than fracture induced currents have failed. We therefore interpret these current measurements as evidence for charge separation across the crack tip during and following fracture. Note that for such currents to be sustained for any length of time during fracture, the circuit must contain relatively high resistance conduction paths. Impurity segregation at grain boundaries and crack branching into the sample bulk may contribute to the effective resistance of the near surface region.

In our investigation of the possible role of chemistry on the emissions during the fracture event itself, we performed photon and radio frequency emission measurements on deuterated and hydrogenated Ti samples in air. Figure 11 shows typical results for TiD_x. The radio frequency emission in air was essentially the same as in vacuum, but the photon emission was much larger, saturating the photomultiplier for approximately 100 μs. A rough estimate of the ratio of intensities of the fast photon emission in air versus vacuum is 10^3. Similar tests performed in N_2 and O_2 atmospheres resulted in very

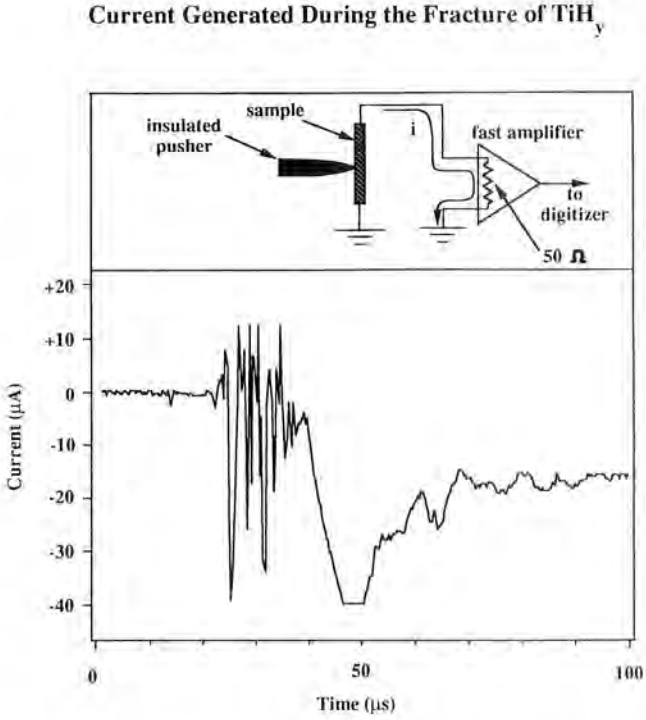

FIG. 10. Fracture-induced current produced in a TiH_y specimen fractured in three point bend. Schematic of circuit is shown in inset.

weak photon emission in N_2 and very strong photon emission in O_2. Tests of undeuterated Ti tensile specimens in an O_2 atmosphere displayed much weaker photon emission during fracture than the deuterated Ti. Suspecting that D_2 would be the dominant species in the crack during fracture, we fractured three point bend deuterated specimens in vacuum near the ionizer of a quadrupole mass spectrometer tuned to mass 4. The background pressure in the vacuum system before fracture was 3×10^{-9} Torr. Figure 12 shows the resulting mass 4 signal. (The ion detector output has passed through a fast electrometer undergoing some integration; thus a smooth curve.) This is a very strong signal (total detected mass 4 corresponds to $\sim 10^{13}$ molecules) which we attribute to D_2 emission (*not* ^{4}He!). Much of this D_2 would be available for a catalytic reaction with O_2 from the air. Thus, it appears that the intense photon emission from TiD_x (and TiH_y) during fracture in air is chemical in origin, not associated with discharges, but due to the catalytic reaction of D_2 from the sample and O_2 from the atmosphere. The highly exothermic nature of the $D_2 + O_2$ reaction, coupled with high reaction rates due to the catalytic nature of the surface, produce intense photon emission in the visible region, possibly black body radiation. (This effect was utilized in the so-called "Doebereiner cigarette lighter".[31]) Using an optical multichannel analyzer, we were able to detect a weak spectrum from one TiD_x sample fractured in air; it appears to be band-like starting up at ~350 nm and extending toward the red to ~650 nm.

SEM photographs of the fracture surface of a TiD_x specimen are shown in Fig. 13. There appears to be evidence of platelet formation of the deuteride phase and intergranular fracture similar to that described by Boyd in Ti–Al alloys.[32] Livanov *et al.*[33] describe the fracture of embrittled Ti as involving the interface between metallic Ti and the hydride including formation of Griffith cracks at the interface whose growth is facilitated by a smaller surface energy compared to the original metal.

Impurity segregation at grain boundaries is a well-known phenomenon and could contribute to the charge separation and inhibition of reneutralization. Mayer *et al.*[7] have also suggested that other mechanisms, including crack branching, could increase the conduction path lengths and resistivity and therefore increase the resistance to charge flow. In the photographs of Fig. 13, one can also see evidence of a few cracks normal to the fracture surface which may also represent interfacial failure at the boundaries of the deuteride platelets.

It was our assumption (and still is) that the phenomena presented so far resulting from TiD_x fracture should be reproduced by similar TiH_y samples. The TiH_y samples (where $y \sim 1.0$) were found to be considerably weaker and more brittle than the TiD_x specimens. We attribute this difference to the higher loading of hydrogen (20% higher). The differences in the fracto-emission between these two types of specimens were astounding. The intensities were dramatically reduced in the TiH_y samples. For example, Fig. 14 shows negative charge emission from the fracture of TiH_y under conditions comparable to Fig. 6(a). The photon emission from the TiH_y samples was barely detectable above the noise. No chemisorptive electron emission or luminescence of a magnitude comparable to that from deuterated Ti was seen. Finally, most surprising was the lack of any detectable mass 2 (H_2) when the TiH_y was fractured in the mass spectrometer system. We are somewhat puzzled by these results although sample strength and the mode of failure may indeed be primary differences. The very small chemisorptive electron emission and luminescence signals suggest that in $TiH_{1.0}$, Ti metal sites are not produced in significant numbers relative to $TiD_{0.8}$. Furthermore, the lack of H_2 emission from $TiH_{1.0}$ suggests that the mass 4 signal (which we attribute to D_2) is not due to molecular deuterium trapped in voids in the metal, but rather from the decomposition of TiD_x during crack propagation. The weaker TiH_y may not release sufficient energy at the crack tip to free the H from its bond with Ti.

IV. CONCLUSION

This preliminary study has shown that both negative and positively charged particles, visible photons, and long wavelength emission are emitted during and fol-

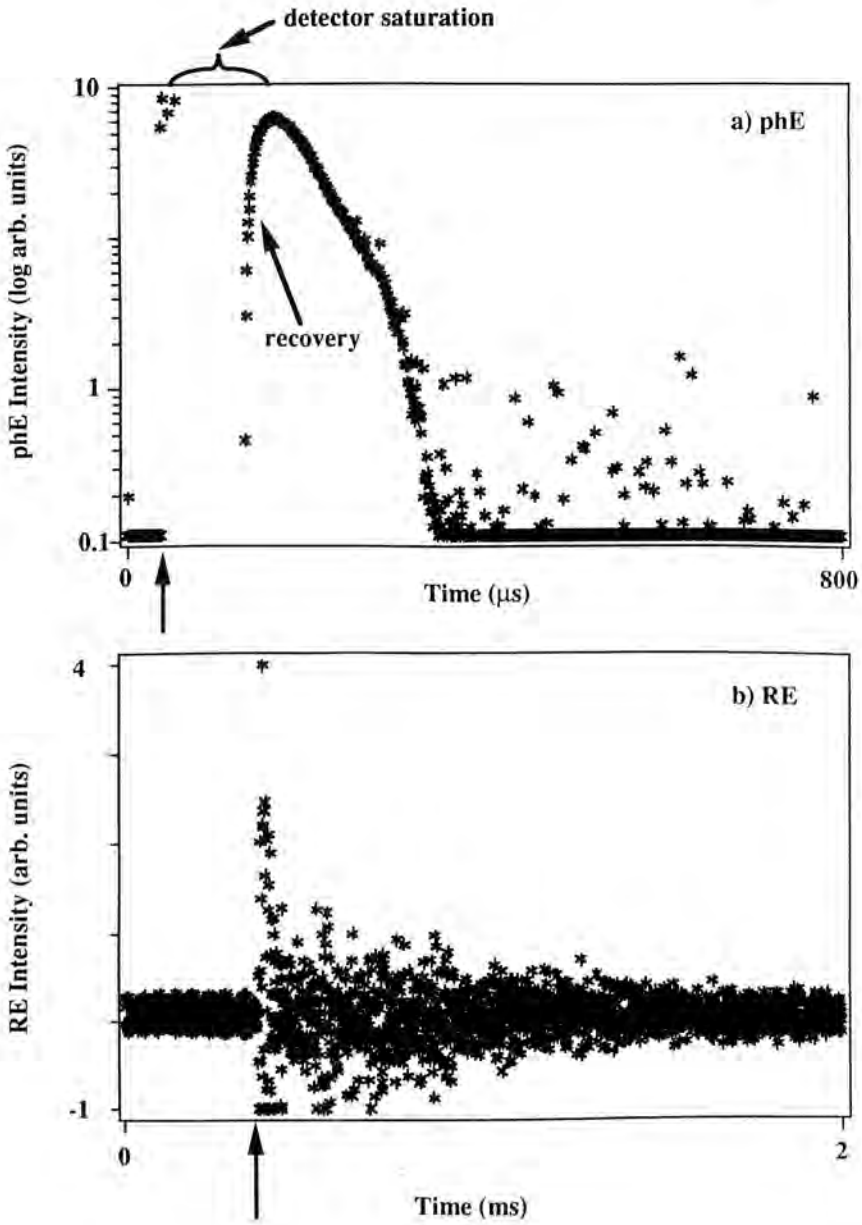

FIG. 11. Simultaneous measurements of the (a) photon emission (phE) and (b) radio frequency emission (RE) produced by fracture of TiD_x in air. The photon emission is three orders of magnitude or more greater in air than in vacuum.

lowing fracture. Surface reactions of freshly exposed Ti with active background gas(es) result in chemisorptive emission of negative and positive charge as well as photons on timescales of seconds. These slow emissions appear to have little relevance to questions of charge separation. The origin of the fast emissions accompanying fracture is not yet clear. However, the behavior of the measured radio frequency emission and fracture-generated currents strongly suggest charge separation during fracture. Further studies will concentrate on determining the identity of the emitted species (e.g., electrons, ±ion and neutral masses), the energy of the charged particles, and spectra of the photon emission in vacuum and in controlled gaseous environments (N_2, O_2, H_2). Most relevant to fracto-fusion mechanisms are (a) the identification of D^+ in the positive charge emission and (b) energy measurements of the charged particles. Electrostatic acceleration would be the only reasonable source of charged particle kinetic energies of several eV or higher. Finally, the dependence of the fracto-emission behavior on materials properties [nature of grain boundaries, locus of fracture, impurity concentrations, D (or H) concentrations] should also be investigated, in particular regarding the observed dif-

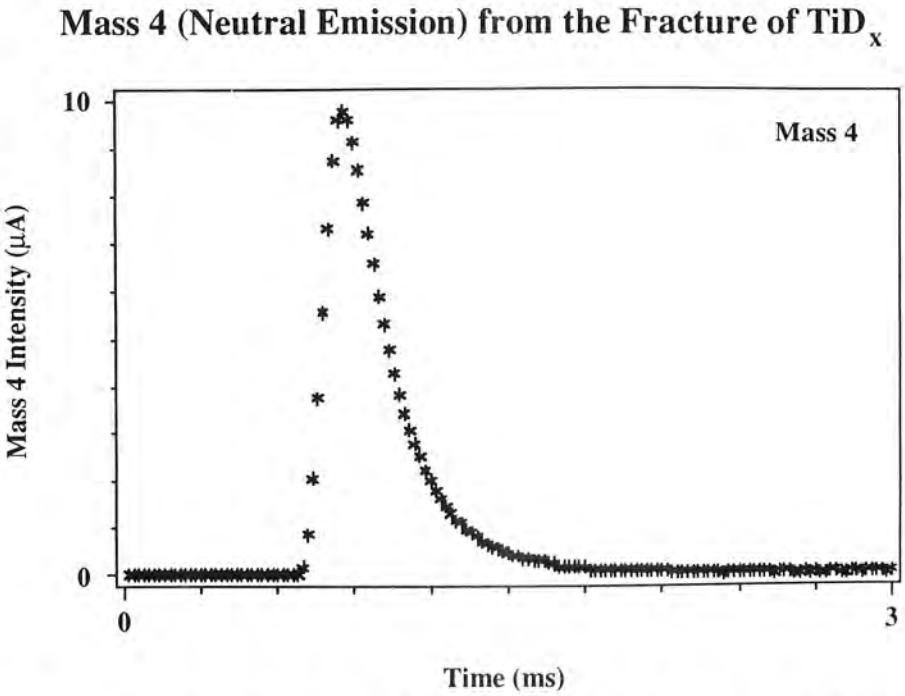

FIG. 12. The quadrupole mass spectrometer output at mass 4 due to the fracture of TiD_x. We attribute this signal to the emission of D_2.

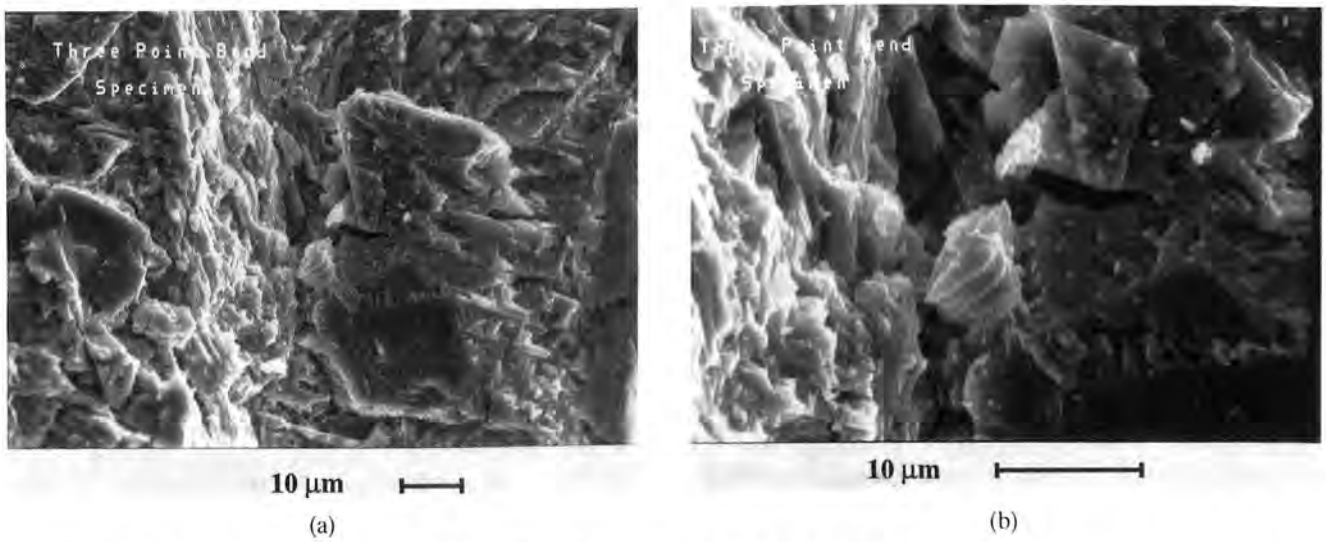

(a) (b)

FIG. 13. SEM photographs of the fracture surface of a TiD_x sample broken in three point bend.

ferences in emission from the $TiD_{0.8}$ and $TiH_{1.0}$. When possible, these studies should be made in conjunction with neutron emission experiments, including correlation experiments between fracture, fracto-emission, and neutron emission. Obviously, if the fracto-fusion mechanism is valid, it would not be a cold fusion process due to the necessary electrostatic acceleration provided by charge separation. Energetically, this charge separation is driven by mechanical forces transmitted to the crack tip via elastic deformation of the lattice.

ACKNOWLEDGMENTS

This work was supported by the Ceramics and Electronics Materials Division of the National Sciences Foundation DMR-8601281, the Office of Naval Research Contract No. N00014-87-K-0514, and the Washington Technology Center. The authors wish to thank Gary Collins, Washington State University, for useful discussions. We also thank M. Stout and A. Geltmacher, Los Alamos National Laboratory, for taking the SEM micrographs of the TiD_x fracture surfaces.

NOTE ADDED IN PROOF

Another discussion of the fracto-fusion mechanism has recently been published: "Fracto-Fusion Mechanism", Tatsuoki Tekeda and Tomonori Takizuka, J. Phys. Soc. Japan **58**, 3073 (1989).

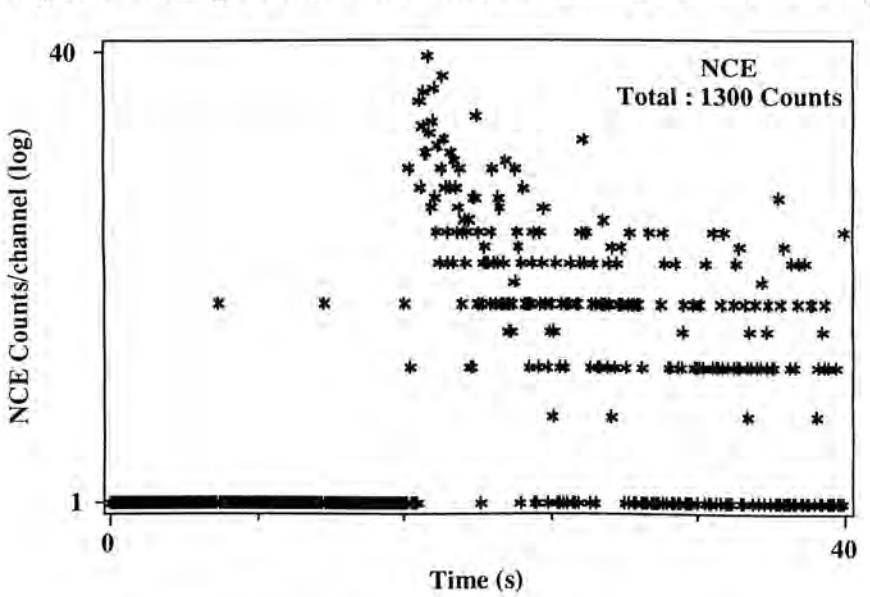

FIG. 14. The negative charge emission from the much weaker, more brittle TiH_y fracture. This emission should be compared with Fig. 6(a) for TiD_x.

A recent experiment has been reported by B.V. Derjaguin, A.G. Lipson, V.A. Kluev, Dm. M. Sakov, and Yu. P. Toporov, Nature **341**, 492 (1989), claiming low levels of neutron emission above background during ball-milling of Ti and deuterium containing compounds. This emission is attributed to a fracto-fusion mechanism.

REFERENCES

[1]M. Fleischmann and S.J. Pons, J. Electroanal. Chem. **261**, 301 (1989).

[2]S.E. Jones, E.P. Palmer, J.B. Czirr, D.L. Decker, G.L. Jensen, J.M. Thorpe, S.F. Taylor, and J. Rafelki, Nature **338**, 737 (1989).

[3]A. De Ninno, A. Frattolillo, G. Lollobattista, L. Martinis, M. Martone, L. Mori, S. Podda, and F. Scaramuzzi, Europhysics Letters **9**, 221 (1989).

[4]H.O. Menlove, M.M. Fowler, E. Garcia, A. Mayer, M.C. Miller, R.R. Ryan, and S.E. Jones, submitted to Nature.

[5]R. Ryan, M. Fowler, E. Garcia, H. Menlove, M. Miller, A. Mayer, J. Wilhelmy, C. Orth, S. Schmidt, D. Moore, A. Voter, and J.T. Dickinson, presented at Santa Fe Workshop on Cold Fusion Phenomena, Santa Fe, NM, May 23–25, 1989.

[6]J.S. Cohen and J.D. Davies, Nature **338**, 705 (1989).

[7]F.J. Mayer, J.S. King, and J.R. Reitz, presented at Santa Fe Workshop on Cold Fusion Phenomena, Santa Fe, NM, May 23–25, 1989.

[8]H. Furth, S. Bernabei, S. Cowley, and R. Kulsrud, Bull. Am. Phys. Soc. **34**, 1860 (A) (1989).

[9]S.E. Segre, S. Atzeni, S. Briguglio, and F. Romanelli, "A Mechanism for Neutron Emission from Deuterium Trapped in Metals" (to be published).

[10]V.A. Klyuev, A.G. Lipson, Yu. P. Toporov, B.V. Deryagin, V.I. Lushchikov, A.V. Strelkov, and E.P. Shabalin, Pis'ma Zh. Tekh. Fiz. **12**, 1333 (1986) [Sov. Tech. Phys. Lett. **12**, 551 (1987)].

[11]B.V. Deryagin, V.A. Klyuev, A.G. Lipson, and Yu. P. Toporov, Kolloidnii Zhurnal **48**, 12 (1986).

[12]J.T. Dickinson, E.E. Donaldson, and M.K. Park, J. Mater. Sci. **16**, 2897 (1981).

[13]J.T. Dickinson, L.C. Jensen, and A. Jahan-Latibari, J. Vac. Sci. Technol. **A2**, 1112 (1984).

[14]J.T. Dickinson, W.D. Williams, and L.C. Jensen, J. Am. Ceram. Soc. **68**, 235 (1985).

[15]J.T. Dickinson, in *Adhesive Chemistry — Developments and Trends*, edited by L.H. Lee (Plenum Publishers, New York, 1984), pp. 193–243.

[16]L.A. K'Singam, J.T. Dickinson, and L.C. Jensen, J. Am. Ceram. Soc. **68**, 510 (1985).

[17]J.T. Dickinson and E.E. Donaldson, J. Adhesion **24**, 199 (1987).

[18]J.T. Dickinson, to appear in *Advances in Adhesion*, edited by L.H. Lee (Plenum Press, New York).

[19]J.T. Dickinson and L.C. Jensen, J. Polym. Sci.: Polym. Phys. Ed. **23**, 873 (1985).

[20]R. Chen and Y. Kirsch, *Analysis of Thermally Stimulated Processes* (Pergamon Press, Oxford, 1981).

[21]J.T. Dickinson, P.F. Braunlich, L.A. Larson, and A. Marceau, Appl. Surf. Sci. **1**, 515 (1978).

[22]D.L. Doering, T. Oda, J.T. Dickinson, and P. Braunlich, Appl. Surf. Sci. **3**, 196 (1979).

[23]B. McCarroll, J. Chem. Phys. **50**, 4758 (1969).

[24]B. Kasemo, Phys. Rev. Lett. **32**, 1114 (1974).

[25]I.V. Krylova, *Proc. 5th Int. Symp. on Exoelectron Emission and Dosimetry*, edited by A. Bohun and A. Scharmann, 40 (1976).

[26]M.A. Loudiana, J. Bye, J.T. Dickinson, and D.A. Dickinson, Surf. Sci. **157**, 459 (1985).

[27]J.K. Norskov, D.M. Newns, and B.I. Lundqvist, Surf. Sci. **80**, 179 (1979).

[28]B. Kasemo, E. Tornqvist, and L. Wallden, Mater. Sci. Eng. **42**, 23 (1980).

[29]R.H. Prince, R.M. Lambert, and J.S. Foord, Surf. Sci. **107**, 605 (1981).

[30]D. Born and E. Linke, *Proc. 5th Int. Symp. on Exoelectron Emission and Dosimetry*, edited by A. Bohun and A. Scharmann, 265–269 (1976).

[31]Cited on BITNET, April 26, 1989, SCHWARTZ_GERHARD @ FRANKFT.

[32]J.D. Boyd, in *The Science, Technology, and Application of Titanium*, edited by R.I. Jaffee and N.E. Promisel (Pergamon Press, Oxford, 1970), pp. 545–555.

[33]V.A. Livanov, B.A. Kolachev, and A.A. Buhanova, in *The Science, Technology, and Application of Titanium*, edited by R.I. Jaffee and N.E. Promisel (Pergamon Press, Oxford, 1970), pp. 561–576.